A novel RNN applied to motion control of mobile robots with criteria optimization and physical constraints[☆]

Abstract

Conventional solutions for the motion control of mobile robots in the unified framework of recurrent neural networks (RNNs) are difficult to consider both criteria optimization and physical constraints. To overcome this limitation, this paper proposes a novel inequality and equality constrained optimization RNN (IECORNN) to handle the motion control of mobile robots. Firstly, the real-time motion control problem with both criteria optimization and physical constraints is skillfully converted to a real-time equality system by leveraging the Lagrange multiplier rule. Then, the detailed design process for the proposed IECORNN is presented. Afterward, theoretical analyses on the motion control problem conversion equivalence, global stability, and exponential convergence property are rigorously provided. Finally, numerical experiment verifications and extensive comparisons based on the mobile robot for two different path-tracking applications sufficiently demonstrate the effectiveness and superiority of the proposed IECORNN for the real-time motion control of mobile robots with both criteria optimization and physical constraints.

Keywords: Recurrent neural networks (RNNs), motion control, mobile robots, criteria optimization, physical constraints.
2010 MSC: 62G35, 92B20, 93B51

1. Introduction

Due to the mobility, flexibility and wide working space, mobile robots are able to complete various complicated motion control tasks, which are similar to the cases of complex motion performed by human with legs and arms [1–4]. Many practical applications in different fields such as industrial manufacture [5], military organizations [6], and public service communities [7] can be ascribed to the motion control of mobile robots. In the recent years, the motion control of mobile robots has been a heated topic for robotic research [8–13]. For examples, Yan *et al.* [11] introduced several modified zeroing neural network models for the motion control of mobile robots by considering the non-convex activation functions as well as accelerating the convergence process with finite-time property. In addition, Kapitanyuk *et al.* [13] developed a new scheme for the path-tracking control of nonholonomic mobile robots on the basis of the guiding vector field strategy. As for the practical applications of mobile robots, most tasks excused by the manipulator end-effector are in Cartesian space while mobile robot actuators work in manipulator joint space in real time [14, 15]. Involving with the characteristics of multiple solutions, nonlinearity, and real-time computation, the motion control of mobile robots is an intensively tough issue to be directly solved [16].

Performance index (or to say, criteria) optimization strategy on the basis of the dynamical quadratic program (DQP) [17] has been an alternative while solving the motion control of mobile robots with some feasible solutions presented in existing studies [18–20]. For examples, Zhang *et al.* [19] introduced an effective time-variant constrained repetitive motion generation approach to achieve the repetitive motion control for humanoid robots by formulating the model as a DQP, and solved by neural networks. In addition, Li *et al.* [20] developed a novel repetitive motion control approach to handle the limitations imposed by external noises by considering the inherent noise suppression capability with the formulation of DQP. Guo *et al.* [21] presented and investigated a new motion control approach with both joint velocity and joint acceleration minimization to address the problem of high joint velocity as well as acceleration for redundant robot manipulators with the DQP

formulation and neural network solver. However, it has been proven that the above solutions via the optimization scheme on the basis of the DQP only possess the asymptotic convergence property [22]. Therefore, new solutions considering criteria optimization with superior convergence property are much more desirable and significant for the real-time motion control of mobile robots.

Physical constraints are usually required to be considered during the motion control of mobile robots. Each practical robots would have physical constraints in each application [22, 23]. In addition, high joint control values without upper or lower bound would wear out the mobile robot structure, and heavily excite its resonance frequencies [24]. Additionally, joint control signals with bounded values are desirable in control process for their similarity to human joints movements and to limit robot vibrations so that the mobile robot life-span would be expanded. Therefore, the solutions for practical mobile robots in motion control with physical constraints are imperative, and many studies have been reported on this issues [22, 25]. For examples, a new dual neural network model for real-time redundancy resolution of redundant robot manipulators was introduced in [22] by considering the physical constraints such as joint angle as well as velocity limits into the DQP problem formulation. In additions, Zhang and Zhang [25] developed an effective varying joint velocity limits constrained minimum-velocity-norm strategy for motion control of redundant robot manipulators by considering the physical constraints of robots as the joint limits. Although physical constraints are ubiquitous for motion control of robots, the above solutions are all limited to the DQP formulations and solutions with asymptotic convergence property.

Differing from the traditional methodologies for motion control problems solving of robot such as adaptive control [26–30], fuzzy control [31–33], and robustness control [34–37], the neural network control [38–46] explores many benefits brought by advanced mobile robots in modern industry. Among various kinds of neural network control strategies, the Hopfield-type recurrent neural networks (RNNs) have been powerful alternatives for the real-time motion control of mobile robots [47–50]. For examples, Li [47] systematically developed and investigated a finite time convergent and noise tolerant RNN for solving the matrix inversion matrix inversion under different kinds of external noises with application to motion control of serial robot manipulators. In addition, Lu *et al.* [48] introduced a new RNN to address the time-variant underdetermined linear system under the influence of noises with double-bound limits of residual errors as well as state variables. Xiao *et al.* [49]

developed a novel framework of special kinds of RNN called zeroing neural network for handling the time-variant quadratic optimization with finite-time convergence property under the influence of different kinds of additive noises. However, there still exists a bottleneck in conventional RNNs (CRNNs). That is the solutions or models via CRNNs are difficult to consider both the criteria optimization subject to the physical constraints during the motion control of mobile robots.

To break the above mentioned bottleneck in the motion control of mobile robot, this paper mainly overcome the limitation that the solutions via CRNNs are hard to consider both criteria optimization and physical constraints. A novel inequality and equality constrained optimization RNN (IECORNN) is proposed in this paper to handle the motion control of mobile robot. The real-time motion control problem with both criteria optimization and physical constraints is skillfully converted to a real-time equality system by using the Lagrange multiplier rule. Then, the detailed design process for the proposed IECORNN is introduced. Afterward, theoretical analyses on the motion control problem conversion equivalence, global stability and exponential convergence property are rigorously provided. Numerical experiment verifications and extensive comparisons based on the mobile robot for two different path-tracking applications sufficiently demonstrate the effectiveness and superiority of the proposed IECORNN for the real-time motion control of mobile robot with both criteria optimization and physical constraints.

The remainder of the paper is organized in four sections. Section 2 presents the preliminaries for the motion control of mobile robots. In Section 3, the IECORNN is proposed with detailed design process and theoretical analyses. Section 4 presents the numerical experiment verifications by two different path-tracking applications as well as comprehensive comparisons. Section 5 concludes the paper with final remarks. The main contributions and novelty of the paper are highlighted as follows.

- To overcome the limitation of CRNNs solutions, this paper proposes a novel IECORNN for the motion control of mobile robot by considering both criteria optimization and physical constraints. This is the first work to handle both the criteria optimization and physical constraints of mobile robot in a unified framework of RNN achieving desirable motion control performance.

- By leveraging the Lagrange multiplier rule, the real-time motion control problem of mobile robot with both criteria optimization and physical

constraints is skillfully converted to a real-time equality system.

- Theoretical analyses on the motion control problem conversion equivalence, global stability and exponential convergence property are rigorously provided with the numerical verification.

2. Preliminaries for motion control of mobile robots

The integrated kinematics of mobile robots at velocity level is presented in this section. Afterwards, the corresponding motion control problem of mobile robots is formulated with the solution via CRNN given. For convenience of further investigation, the nomenclature is presented.

Nomenclature

$f(\cdot,\cdot)$	Continuous-and-nonlinear forward-kinematics mapping of mobile robots
$\Theta(t)$	Combined-angle vector of mobile robot
Θ^-	Lower bound of physical constraints of combined-angle vector
Θ^+	Upper bound of physical constraints of combined-angle vector
$\dot{\Theta}(t)$	Combined-velocity vector of mobile robot
$\varphi(t)$	Rotational-angle vector of left as well as right wheels
$\dot{\varphi}(t)$	Rotational-velocity vector of left as well as right wheels
$\theta(t)$	Joint-angle vector of mobile robot manipulators
$\mathbf{r}_{\mathrm{m}}(t)$	End-effector 3D position vector in Cartesian space
$\dot{\mathbf{r}}_{\mathrm{m}}(t)$	End-effector 3D velocity vector in Cartesian space
$\mathcal{M}(\cdot,\cdot)$	Integration matrix of the geometrical relation information of both mobile base and manipulator
$\phi(t)$	Heading angle of mobile base defined by angle measured from X-axis to symmetry axis of a mobile base

2.1. Problem description and CRNN solution

The forward kinematics modelling of mobile robots is described as

$$f(\Theta(t),t)=\mathbf{r}_{\mathrm{m}}(t), \tag{1}$$

where $f(\cdot,\cdot):\mathbb{R}^{2+n}\rightarrow\mathbb{R}^{m}$, vector $\Theta(t)\in\mathbb{R}^{2+n}$ defined as $\Theta(t)=[\varphi^{\mathrm{T}}(t),\theta^{\mathrm{T}}(t)]^{\mathrm{T}}$ with $\varphi(t)=[\varphi_{\mathrm{l}}(t),\varphi_{\mathrm{r}}(t)]^{\mathrm{T}}\in\mathbb{R}^{2}$, and $\mathbf{r}_{\mathrm{m}}\in\mathbb{R}^{m}$ being defined in the nomenclature.

Note that the physical modeling of mobile robot investigated in the paper is an integration of a mobile base and a 6-joint 3-dimensional (3D) manipulator. On the basis of the related kinematics modeling of mobile robot in [16], the integrated-kinematics equation at velocity level corresponding to the world-coordinate system is described as the following compact-matrix form:

$$\dot{\mathbf{r}}_{\mathrm{m}}(t) = \mathcal{M}(\phi(t), \theta(t))\dot{\Theta}(t) \tag{2}$$

with $\dot{\mathbf{r}}_{\mathrm{m}}(t) \in \mathbb{R}^m$ being the time derivative of $\mathbf{r}_{\mathrm{m}}(t)$. In addition, the detailed formulation of augmented matrix $\mathcal{M}(\phi(t), \theta(t)) \in \mathbb{R}^{m\times(2+n)}$ can be referred to [16]. The time derivative of combined-velocity vector $\dot{\Theta}(t) \in \mathbb{R}^{2+n}$ is defined as $\dot{\Theta}(t) = [\dot{\varphi}(t)^{\mathrm{T}}, \dot{\theta}(t)^{\mathrm{T}}]^{\mathrm{T}}$ with $\dot{\varphi}(t) = [\dot{\varphi}_{\mathrm{l}}(t), \dot{\varphi}_{\mathrm{r}}(t)]^{\mathrm{T}} \in \mathbb{R}^2$ being defined in nomenclature.

If a desired (or to say, user-defined) path $\mathbf{r}_{\mathrm{md}}(t) \in \mathbb{R}^m$ is considered to be tracked by an end-effector of the mobile robot in time t, then the following description can be obtained:

$$f(\Theta, t) = \mathbf{r}_{\mathrm{m}}(t) \rightarrow \mathbf{r}_{\mathrm{md}}(t). \tag{3}$$

For the time derivative of equation (3), the integrated-kinematics equation (2) at the velocity level is exactly obtained as below:

$$\mathcal{M}(\phi(t), \theta(t))\dot{\Theta} = \dot{\mathbf{r}}_{\mathrm{m}}(t) \rightarrow \dot{\mathbf{r}}_{\mathrm{md}}(t) \tag{4}$$

with $\dot{\mathbf{r}}_{\mathrm{md}}(t) \in \mathbb{R}^m$ being the time derivative of a desired (or to say, user-defined) path $\mathbf{r}_{\mathrm{md}}(t)$. Specifically, provided a desired path $\mathbf{r}_{\mathrm{md}}(t)$ of end-effector on mobile robot, a feasible solution that generates the corresponding joint-and-wheel trajectories in time t has to be found. This is a general problem description for the motion control of mobile robots.

By simply defending a vector value error function $\mathbf{e}(t) = \mathbf{r}_{\mathrm{m}}(t) - \mathbf{r}_{\mathrm{md}}(t)$ and also utilizing the neural dynamical design formula $\dot{\mathbf{e}}(t) = -\zeta\Upsilon(\mathbf{e}(t))$, it can be readily obtained a CRNN as below:

$$\mathcal{M}(\phi(t), \theta(t))\dot{\Theta} = \dot{\mathbf{r}}_{\mathrm{md}}(t) - \gamma\Upsilon(\mathbf{r}_{\mathrm{m}}(t) - \mathbf{r}_{\mathrm{md}}(t)), \tag{5}$$

where parameter γ denoting the predefined parameter of the neural network for user to adjustment the convergence rate, and $\Upsilon(\cdot) : \mathbb{R}^{n+m+p} \rightarrow \mathbb{R}^{n+m+p}$ denoting an activation-function vector mapping with each element being a monotonically-increasing odd function. However, it can be found that such a CRNN can not consider other criteria optimization or physical constraints during the mobile robot motion control.

2.2. Criteria optimization and physical constraints

Being quite different form the problem description (4) of motion control of mobile robot in a unified framework of RNN considers neither the criteria optimization nor the physical constraints. In some practical applications, a mobile robot is required to minimize velocity norm for energy dissipation reduction. There, a criteria optimization is formulated as follows:

$$\text{min. } \frac{\|\dot{\Theta}(t)\|_{\mathrm{E}}^2}{2}, \tag{6}$$

where $\|\cdot\|_{\mathrm{E}}$ denotes the Euclidean norm of a vector.

Moreover, physical constraints of the control signals are required to be considered at the same time during the motion control process as below:

$$\dot{\Theta}^{-} \leq \dot{\Theta}(t) \leq \dot{\Theta}^{+}. \tag{7}$$

Therefore, a more practical description for the motion control of mobile robots with both criteria optimization and physical constraints can be described as follows:

$$\begin{aligned} &\text{min. } \frac{\|\dot{\Theta}(t)\|_{\mathrm{E}}^2}{2} \\ &\text{s. t. } \mathcal{M}(\phi(t),\theta(t4))\dot{\Theta}(t) = \dot{\mathbf{r}}_{\mathrm{md}}(t) - \gamma\Upsilon(\mathbf{r}_{\mathrm{m}}(t) - \mathbf{r}_{\mathrm{md}}(t)), \\ &\qquad \dot{\Theta}^{-} \leq \dot{\Theta}(t) \leq \dot{\Theta}^{+}. \end{aligned} \tag{8}$$

The above problem description (8) for motion control of mobile robots is quite different from those in previous works [16, 18], which is able to simultaneously consider optimization objective and physical constraints in more practical applications.

3. IECORNN design and theoretical analyses

As the preliminaries of the work, problem formulations for the motion control of mobile robots and the conventional solution via CRNN are presented in Section 2. In this section, a novel IECORNN is proposed by consideration of both criteria optimization and physical constraints of mobile robot. In addition, theoretical analyses on motion control problem conversion equivalence, global stability and exponential convergence are rigorously provided.

3.1. IECORNN design

The motion control problem (8) of mobile robots with both criteria optimization and physical constraints can be equivalently reformulated as the following vector form of time-variant nonlinear optimization subject to both inequality and equality constraints:

$$\begin{aligned} &\min\ \mathcal{F}(\dot{\Theta}(t),t) \\ &\text{s. t. } \mathbf{h}(\dot{\Theta}(t)) = A(t)\dot{\Theta}(t) + \mathbf{b}(t) = 0, \\ &\quad \mathbf{g}(\dot{\Theta}(t)) = C(t)\dot{\Theta}(t) + \mathbf{d}(t) \leq 0, \end{aligned} \tag{9}$$

where optimization objective function $\mathcal{F}(\Theta(t),t) = \|\dot{\Theta}(t)\|_{\mathrm{E}}^2/2$, and $\mathbf{h}(\dot{\Theta}(t)) \in \mathbb{R}^m$ and $\mathbf{g}(\dot{\Theta}(t)) \in \mathbb{R}^p$ are the equality constraint and inequality constraints, respectively, with the rank of $A(t) = \mathcal{M}(\phi(t),\theta(t)) \in \mathbb{R}^{m\times n}$ being always equal to m, and vector $\mathbf{b}(t) = -\dot{\mathbf{r}}_{\mathrm{md}}(t) + \gamma\Upsilon(\mathbf{r}_{\mathrm{m}}(t) - \mathbf{r}_{\mathrm{md}}(t)) \in \mathbb{R}^m$, matrix $C(t) = [I,\ -I]^{\mathrm{T}} \in \mathbb{R}^{p\times n}$ and vector $\mathbf{d}(t) = [(\dot{\Theta}^+)^{\mathrm{T}},\ (-\dot{\Theta}^-)^{\mathrm{T}}]^{\mathrm{T}} \in \mathbb{R}^p$. The goal of time-variant nonlinear optimization with multiple constraints is to find a feasible solution $\dot{\Theta}(t)$ such that (9) holds true at any time instant $t \in [0,+\infty)$.

According to the Lagrange multiplier rule [51], to find a feasible solution $\dot{\Theta}(t)$ of nonlinear optimization (9), a Lagrange function is defined as follows:

$$\mathbb{L}(\dot{\Theta}(t),\alpha(t),\beta(t),t) = \mathcal{F}(\dot{\Theta}(t),t) + \sum_{i=1}^{m}\alpha_i(t)h_i(\dot{\Theta}(t)) + \sum_{j=1}^{p}\beta_j(t)g_j(\dot{\Theta}(t)), \tag{10}$$

where $\alpha(t) = [\alpha_1(t),\alpha_2(t),\cdots,\alpha_m(t)]^{\mathrm{T}} \in \mathbb{R}^m$, and $\beta(t) = [\beta_1(t),\beta_2(t),\cdots,\beta_p(t)]^{\mathrm{T}} \in \mathbb{R}^p$ are the Lagrange multipliers that correspond to equality constraint and inequality constraint, respectively. Equation (10) can be rewritten as a vector form as follows:

$$\begin{aligned} \mathbb{L}(\dot{\Theta}(t),\alpha(t),\beta(t),t) =& \mathcal{F}(\dot{\Theta}(t),t) + \alpha^{\mathrm{T}}(t)(A(t)\dot{\Theta}(t) + \mathbf{b}(t)) \\ &+ \beta^{\mathrm{T}}(t)(C(t)\dot{\Theta}(t) + \mathbf{d}(t)), \end{aligned} \tag{11}$$

Based on the theoretical results in the Lagrange multiplier rule [51], to solve the time-variant of nonlinear optimization (9) subject to inequality and equality constraints is equal to solve the following time-variant of nonlinear optimization without constraints:

$$\min_{\dot{\Theta}(t),\alpha(t),\beta(t)} \mathbb{L}(\dot{\Theta}(t),\alpha(t),\beta(t),t). \tag{12}$$

Then, the solution $\dot{\Theta}(t)$ to the time-variant nonlinear optimization (9) is found by solving the following set of equations:

$$\begin{cases} \nabla_{\dot{\Theta}}\mathbb{L} = \frac{\partial \mathbb{L}(\dot{\Theta}(t),\alpha(t),\beta(t),t)}{\partial \dot{\Theta}} = 0, \\ \nabla_{\alpha}\mathbb{L} = \mathbf{h}(\dot{\Theta}(t)) = 0, \\ \mathbf{g}(\dot{\Theta}(t)) \leq 0, \beta(t) \geq 0, \text{ and } \beta^{\mathrm{T}}(t)\mathbf{g}(\dot{\Theta}(t)) = 0, \end{cases} \tag{13}$$

that is

$$\begin{cases} \frac{\partial \mathcal{F}(\dot{\Theta}(t),t)}{\partial \dot{\Theta}} + A^{\mathrm{T}}(t)\alpha(t) + \left(\frac{\partial \mathbf{g}(\dot{\Theta}(t))}{\partial \dot{\Theta}}\right)^{\mathrm{T}} \beta(t) = 0, \\ \mathbf{h}(\dot{\Theta}(t)) = 0, \\ \mathbf{g}(\dot{\Theta}(t)) \leq 0, \beta(t) \geq 0, \text{ and } \beta^{\mathrm{T}}(t)\mathbf{g}(\dot{\Theta}(t)) = 0. \end{cases} \tag{14}$$

In a unified framework of RNN design process, a scalar valued, vector valued, or matrix valued indefinite error function could be initially defined to monitor the time-variant motion control process of the problem involved. As for the time-variant nonlinear optimization problem (9) solving, the following vector valued indefinite error function is thus defined:

$$\epsilon(t) = \begin{bmatrix} \frac{\partial \mathcal{F}(\dot{\Theta}(t),t)}{\partial \dot{\Theta}} + A^{\mathrm{T}}(t)\alpha(t) + \left(\frac{\partial \mathbf{g}(\dot{\Theta}(t))}{\partial \dot{\Theta}}\right)^{\mathrm{T}} \beta(t) \\ -\mathbf{h}(\dot{\Theta}(t)) \\ \digamma^{+}(\mathbf{g}(\dot{\Theta}(t)) + \beta(t)) - \beta(t)) \end{bmatrix} \tag{15}$$

with $\epsilon(t) \in \mathbb{R}^{n+m+p}$. In addition, the ith element of function mapping $\digamma^{+}(\cdot) : \mathbb{R}^{p} \to \mathbb{R}^{p}$ denotes as

$$\digamma_{i}^{+}(v_i(t)) = \begin{cases} v_i(t), & \text{if } \ v_i(t) > 0, \\ 0, & \text{if } \ v_i(t) \leq 0, \end{cases}$$

where $\mathbf{v}(t) \in \mathbb{R}^{p}$ denotes a vector. It can be easily obtained:

$$\frac{\mathrm{d}((\partial \mathbf{g}(\dot{\Theta}(t))/\partial \dot{\Theta})^{\mathrm{T}}\beta(t))}{\mathrm{d}t} = \left(\frac{\partial \mathbf{g}(\dot{\Theta}(t))}{\partial \dot{\Theta}}\right)^{\mathrm{T}} \dot{\beta}(t) + \frac{\mathrm{d}^{\mathrm{T}}(\partial \mathbf{g}(\dot{\Theta}(t))/\partial \dot{\Theta})}{\mathrm{d}t}\beta(t). \tag{16}$$

Note that

$$\frac{\mathrm{d}(\partial \mathbf{g}(\dot{\Theta}(t))/\partial \dot{\Theta})}{\mathrm{d}t} = \sum_{i=1}^{p} \frac{\partial^2 \mathbf{g}(\dot{\Theta}(t))}{\partial \dot{\Theta} \partial \dot{\Theta}_i} \ddot{\Theta}_i(t), \tag{17}$$

always holds true. Thus, one can obtain:

$$\begin{aligned}\frac{\mathrm{d}^{\mathrm{T}}(\partial\mathbf{g}(\dot{\Theta}(t))/\partial\dot{\Theta})}{\mathrm{d}t}\beta(t) &= \sum_{i=1}^{p}\left(\frac{\partial^2\mathbf{g}(\dot{\Theta}(t))}{\partial\dot{\Theta}\partial\dot{\Theta}_i}\ddot{\Theta}_i(t)\beta(t)\right)\\ &= \sum_{i=1}^{p}\ddot{\Theta}_i(t)\left(\frac{\partial^2\mathbf{g}(\dot{\Theta}(t))}{\partial\dot{\Theta}\partial\dot{\Theta}_i}\right)\beta(t).\end{aligned} \tag{18}$$

Let us make a variable substitution as

$$\left(\frac{\partial^2\mathbf{g}(\dot{\Theta}(t))}{\partial\dot{\Theta}\partial\dot{\Theta}_i}\right)\beta(t) = \varphi_i(t), \tag{19}$$

with

$$\Psi(t) = [\varphi_1(t), \varphi_2(t), \cdots, \varphi_i(t), \cdots, \varphi_n(t)]. \tag{20}$$

Thus, we have:

$$\frac{\mathrm{d}^{\mathrm{T}}(\partial\mathbf{g}(\dot{\Theta}(t))/\partial\dot{\Theta})}{\mathrm{d}t}\beta(t) = \sum_{i=1}^{p}\ddot{\Theta}_i(t)\varphi_i(t) = \Psi(t)\ddot{\Theta}(t), \tag{21}$$

which further yields:

$$\frac{\mathrm{d}((\partial\mathbf{g}(\dot{\Theta}(t))/\partial\dot{\Theta})^{\mathrm{T}}\beta(t))}{\mathrm{d}t} = \Psi(t)\ddot{\Theta}(t) + \left(\frac{\partial\mathbf{g}(\dot{\Theta}(t))}{\partial\dot{\Theta}}\right)^{\mathrm{T}}\dot{\beta}(t). \tag{22}$$

To exponentially force the error function (15) converging to zero, it can be employed the dynamical design formula [22, 52] as $\dot{\epsilon}(t) = -\zeta\Upsilon(\epsilon(t))$ with predefined parameter ζ and activation-function vector mapping Υ defined as before. According to the above operation and variable substitution, one can obtain the time-derivative of error function (15) as $\dot{\epsilon}(t) = [\dot{\epsilon}_1(t), \dot{\epsilon}_2(t), \dot{\epsilon}_3(t)]^{\mathrm{T}}$ with $\dot{\epsilon}_1(t) \in \mathbb{R}^n$, $\dot{\epsilon}_2(t) \in \mathbb{R}^m$ and $\dot{\epsilon}_3(t) \in \mathbb{R}^p$ being respective as

$$\begin{aligned}\dot{\epsilon}_1(t) = &\frac{\partial^2\mathcal{F}(\dot{\Theta}(t),t)}{\partial\dot{\Theta}^2}\ddot{\Theta}(t) + \dot{A}^{\mathrm{T}}(t)\alpha(t) + A^{\mathrm{T}}(t)\dot{\alpha}(t)\\ &+ \Psi(t)\ddot{\Theta}(t) + \left(\frac{\partial\mathbf{g}(\dot{\Theta}(t))}{\partial\dot{\Theta}}\right)^{\mathrm{T}}\dot{\beta}(t),\end{aligned} \tag{23}$$

$$\dot{\epsilon}_2(t) = -A(t)\ddot{\Theta}(t) - \dot{A}(t)\dot{\Theta}(t) - \dot{\mathbf{b}}(t), \tag{24}$$

$$\dot{\epsilon}_3(t) = \Phi(t)F^{+}\left(\frac{\partial\mathbf{g}(\dot{\Theta}(t))}{\partial\dot{\Theta}}\ddot{\Theta}(t) + \dot{\beta}(t)\right) - \dot{\beta}(t), \tag{25}$$

where function mapping $\Phi(t) \in \mathbb{R}^{p\times p}$ denotes as below:

$$\Phi(t) = \mathrm{diag}(\chi(\mathbf{g}(\dot{\Theta}(t)) + \beta(t))) \tag{26}$$

with operator $\mathrm{diag}(\mathbf{v}(t)) : \mathbb{R}^p \to \mathbb{R}^{p\times p}$ for generating a $p \times p$ dimensional square matrix with the elements of vector $\mathbf{v}(t) \in \mathbb{R}^p$ on the diagonal, and each element of $\chi(\cdot) : \mathbb{R}^p \to \mathbb{R}^p$ denoting as below:

$$\chi_i(v_i(t)) = \begin{cases} 1, & \text{if } \ v_i(t) > 0, \\ 0, & \text{if } \ v_i(t) \leq 0. \end{cases}$$

Hence, the IECORNN for solving the motion control problem (8) of mobile robots with both criteria optimization and physical constraints is proposed as the following dynamical equation:

$$\begin{aligned} &\begin{bmatrix} Q(t) & A^{\mathrm{T}}(t) & C^{\mathrm{T}}(t) \\ -A(t) & 0 & 0 \\ M(t) & 0 & R(t) \end{bmatrix} \begin{bmatrix} \dot{\Theta}(t) \\ \dot{\alpha}(t) \\ \dot{\beta}(t) \end{bmatrix} \\ &= -\zeta \Upsilon \left(\begin{bmatrix} \epsilon_1(t) \\ \epsilon_2(t) \\ \epsilon_3(t) \end{bmatrix} \right) - \begin{bmatrix} \mathbf{r}_1(t) \\ \mathbf{r}_2(t) \\ \mathbf{r}_3(t) \end{bmatrix}. \end{aligned} \tag{27}$$

Dynamical equation (27) can be reformulated as a compact matrix form as below:

$$\mathcal{W}(t)\dot{\mathbf{s}}(t) = -\zeta \Upsilon(\epsilon(t)) - \mathbf{r}(t), \tag{28}$$

with matrix $\mathcal{W}(t)$ and state vector $\dot{\mathbf{s}}(t)$ being respectively depicted as

$$\mathcal{W}(t) = \begin{bmatrix} Q(t) & A^{\mathrm{T}}(t) & C^{\mathrm{T}}(t) \\ -A(t) & 0 & 0 \\ M(t) & 0 & R(t) \end{bmatrix}, \ \dot{\mathbf{s}}(t) = \begin{bmatrix} \dot{\Theta}(t) \\ \dot{\alpha}(t) \\ \dot{\beta}(t) \end{bmatrix}$$

with matrix $Q(t) = \partial^2 \mathcal{F}(\dot{\Theta}(t), t)/\partial \dot{\Theta}^2 + \Psi(t)$, matrix $M(t) = \Phi(t)C(t)$, matrix $R(t) = \Phi(t) - I$, vector $\mathbf{r}_1(t) = \dot{A}^{\mathrm{T}}(t)\alpha(t)$, vector $\mathbf{r}_2(t) = -\dot{A}(t)\dot{\Theta}(t) - \dot{\mathbf{b}}(t)$, vector $\mathbf{r}_3(t) = 0$ and vector $\mathbf{r}(t) = [\mathbf{r}_1(t), \mathbf{r}_2(t), \mathbf{r}_3(t)]^{\mathrm{T}}$.

A explicit form of the proposed IECORNN (28) can be computability rewritten as follows:

$$\dot{\mathbf{s}}(t) = -\mathcal{W}^{\dagger}(t)(\zeta \Upsilon(\epsilon(t)) + \mathbf{r}(t)), \tag{29}$$

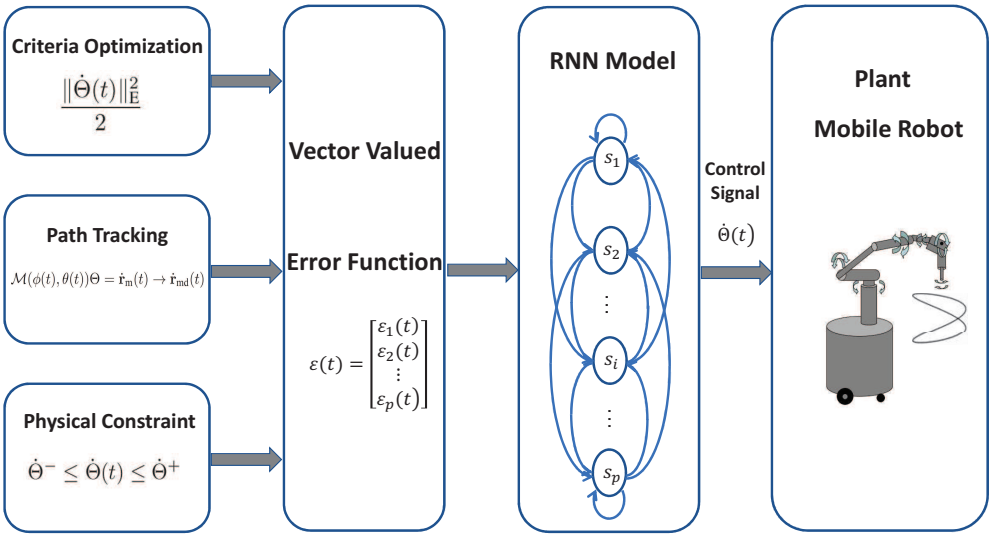

Figure 1: Architecture of the proposed IECORNN (28) applied to the motion control problem (8) of mobile robots with both criteria optimization and physical constraints.

where the ith (with $i = 1, 2, \cdots, n+m+p$) neuron form of the proposed IECORNN depicts as

$$s_i = \int \sum_{j=1}^{p} w_{ij}(-\zeta \Upsilon(\epsilon_i(t)) - r_i(t))\mathrm{d}t, \tag{30}$$

where s_i is the ith state neuron of the IECORNN (28), and w_{ij} is the ijth element of the time-variant weight matrix $\mathcal{W}^{\dagger}(t)$. As it can be readily found that the first n elements of the RNN states $\mathbf{s}(t)$ are the real-time solution of the motion control problem (8) of mobile robot manipulators with both criteria optimization and physical constraints. Actually, the solution is the real-time motion control signals $\dot{\Theta}(t)$. The architecture of the proposed IECORNN (28) for solving the motion control problem (8) of mobile robots with both criteria optimization and physical constraints is illustrated in Fig. 1 for practitioners to intuitively understand main control principle. As shown in Fig. 1, the proposed IECORNN (28) is a typical kind of RNNs, which is able to effectively address the time-variant nonlinear optimization problem with both inequality and equality constraints, and thus readily handle the mobile robot motion control problems.

3.2. Theoretical analyses

In this part, the theoretical analyses on problem conversion equivalence, global stability as well as the convergence property of the proposed IECORN-N (28) for solving the motion control problem (8) of mobile robot manipulators with both criteria optimization and physical constraints. The following literatures, i.e., [22, 52–55] can be supplementary materials for better understanding the preliminaries of the following theoretical analyses. To guarantee the existence of an optimal solution to motion control problem (8), the following two lemmas are provided firstly.

Lemma 1. *[53]: Assumed that there exist two vectors* $\alpha^*(t) \in \mathbb{R}^m$ *and* $\beta^*(t) \in \mathbb{R}^p$*, and the integrated vector* $\mathbf{s}^*(t) = [\dot{\Theta}^{*T}(t), \alpha^{*T}(t), \beta^{*T}(t)]^T \in \mathbb{R}^{n+m+p}$ *satisfies the Karush-Kuhn-Tucker (KKT) condition as below:*

$$\begin{cases} \frac{\partial \mathcal{F}(\dot{\Theta}(t),t)}{\partial \dot{\Theta}}|_{\dot{\Theta}(t)=\dot{\Theta}^*(t)} + A^T(t)\alpha^*(t) + C^T(t)\beta^*(t) = 0, \\ A(t)\dot{\Theta}^*(t) + \mathbf{b}(t) = 0, \\ C(t)\dot{\Theta}^*(t) + \mathbf{d}(t) \leq 0, \beta^*(t) \geq 0, \\ \beta^{*T}(t)(C(t)\dot{\Theta}^*(t) + \mathbf{d}(t)) = 0, \end{cases} \tag{31}$$

vector $\dot{\Theta}^*(t) \in$ *is a KKT point and also an optimal solution to the motion control problem (8) of mobile robot manipulators with both criteria optimization and physical constraints.*

Proof. It can be generalized from [53].

Lemma 2. *[54]: Assumed that time-variant nonlinear optimization objective function* $\mathcal{F}(\dot{\Theta}(t), t)$ *is a time-variant convex at each time instant* t_e*, and the domain of* $\dot{\Theta}(t_e)$ *depicted in* Π_e *is a convex set for each* t_e *for all* $\dot{\Theta}_1(t_e)$*, and* $\dot{\Theta}_2(t_e)$ *in the domain and all* $0 \leq \nu \leq 1$ *for* $\mathcal{F}(\dot{\Theta}(t), t)$ *satisfying the convexity inequality as below:*

$$\begin{aligned} &\mathcal{F}(\nu\dot{\Theta}_1(t_e) + (1-\nu)\dot{\Theta}_2(t_e), t_e) \\ &\leq \nu\mathcal{F}(\dot{\Theta}_1(t_e), t_e) + (1-\nu)\mathcal{F}(\dot{\Theta}_2(t_e), t_e), \end{aligned} \tag{32}$$

for any two points $\dot{\Theta}_1(t_e)$ *and* $\dot{\Theta}_2(t_e)$ *in the domain* Π_e*, and their line segment also belonging to* Π_e*, i.e.,* $\Pi\dot{\Theta}_1(t_e) + (1-\Pi)\dot{\Theta}_2(t_e) \in \Pi_e$ *for all* $0 \leq \Pi \leq 1$*, then vector* $\dot{\Theta}^*(t)$ *is the optimal solution to the motion control problem (8) of mobile robot manipulators with both criteria optimization and physical constraints, if and only if* $\dot{\Theta}^*(t)$ *is a KKT point of (8).*

PROOF. It can be generalized from [54].

Theorem 1. *(Equivalence of Problems Conversion for IECORNN): Assumed that there exist an optimal solution to the motion control problem (8) of mobile robots with both criteria optimization and physical constraints. To solve the set of equations depicted in (14) for problem (8) is equivalent to solving the following set of equality system:*

$$\begin{cases} \frac{\partial \mathcal{F}(\dot{\Theta}(t),t)}{\partial \dot{\Theta}} + A^T(t)\alpha(t) + \left(\frac{\partial \mathbf{g}(\dot{\Theta}(t))}{\partial \dot{\Theta}}\right)^T \beta(t) = 0, \\ \mathbf{h}(\dot{\Theta}(t)) = 0, \\ \digamma^+(\mathbf{g}(\dot{\Theta}(t)) + \beta(t)) = \beta(t), \end{cases} \tag{33}$$

where the ith element of function mapping $\digamma^+(\cdot) : \mathbb{R}^p \to \mathbb{R}^p$ *depicted in*

$$\digamma_i^+(v_i(t)) = \begin{cases} v_i(t), & if \;\; v_i(t) > 0, \\ 0, & if \;\; v_i(t) \leq 0, \end{cases} \tag{34}$$

with $\mathbf{v}(t) \in \mathbb{R}^p$ *denotes a vector, and* $v_i(t)$ *is the* i *the element of* $\mathbf{v}(t)$.

PROOF. That is to prove that to solve

$$\mathbf{g}(\dot{\Theta}(t)) \leq 0, \beta(t) \geq 0, \text{ and } \beta^{\mathrm{T}}(t)\mathbf{g}(\dot{\Theta}(t)) = 0, \tag{35}$$

is equivalent to solve

$$\digamma^+(\mathbf{g}(\dot{\Theta}(t)) + \beta(t)) = \beta(t), \tag{36}$$

which can be divided as the following two part.

In the first part, let us denote vectors $\mathbf{g}(\dot{\Theta}(t))$ and $\beta(t)$ respectively as below:

$$\mathbf{g}(\dot{\Theta}(t)) = \begin{bmatrix} g_1(\dot{\Theta}(t)) \\ g_2(\dot{\Theta}(t)) \\ \vdots \\ g_p(\dot{\Theta}(t)) \end{bmatrix}, \text{ and } \beta(t) = \begin{bmatrix} \beta_1(t) \\ \beta_2(t) \\ \vdots \\ \beta_p(t) \end{bmatrix},$$

with $i = 1, 2, \cdots, p$. Provided that $g_i(\dot{\Theta}(t)) \leq 0$, $\beta_i(t) \geq 0$ as well as $\sum_{i=1}^{p} \beta_i(t) g_i(\dot{\Theta}(t)) = 0$, one can readily obtain:

$$\beta_i(t) g_i(\dot{\Theta}(t)) \leq 0, \; \forall i = 1, 2, \cdots, p, \tag{37}$$

and further leads to

$$\sum_{i=1}^{p} \beta_i(t) g_i(\dot{\Theta}(t)) \leq 0. \tag{38}$$

Note that $\sum_{i=1}^{p} \beta_i(t) g_i(\dot{\Theta}(t)) = 0$ holds true. It can be obtained:

$$\beta_i(t) g_i(\dot{\Theta}(t)) = 0 \tag{39}$$

with $i = 1, 2, \cdots, p$, otherwise $\sum_{i=1}^{p} \beta_i(t) g_i(\dot{\Theta}(t)) < 0$. Thus, one can have: $\beta_i(t) = 0$ or $g_i(\dot{\Theta}(t))$ for all i. *Case 1:* If $\beta_i(t) = 0$, then

$$\digamma_i^+(g_i(\dot{\Theta}(t)) + \beta_i(t)) = \digamma_i^+(g_i(\dot{\Theta}(t))) = \beta_i(t) = 0 \tag{40}$$

with $g_i(\dot{\Theta}(t)) \leq 0$, which makes that (36) can be derived from (35). *Case 2:* If $g_i(\dot{\Theta}(t)) = 0$, then

$$\digamma_i^+(g_i(\dot{\Theta}(t)) + \beta_i(t)) = \digamma_i^+(\beta_i(t)) = \beta_i(t) \tag{41}$$

with $\beta_i(t) \geq 0$, which also makes that (36) can be derived from (35). Part I thus completes.

In the second part, provided that $\digamma^+(\mathbf{g}(\dot{\Theta}(t)) + \beta(t)) = \beta(t)$ with each element being $\digamma_i^+(g_i(\dot{\Theta}(t)) + \beta_i(t)) = \beta_i(t)$ holds true, it has $\beta_i(t) \geq 0$ for $\digamma_i^+(\cdot) \geq 0$ with $i = 1, 2, \cdots, p$. *Case 1:* If $g_i(\dot{\Theta}(t)) + \beta_i(t) \geq 0$, then

$$g_i(\dot{\Theta}(t)) + \beta_i(t) = \beta_i(t) \tag{42}$$

with $\digamma_i^+(g_i(\dot{\Theta}(t)) + \beta_i(t)) = g_i(\dot{\Theta}(t)) + \beta_i(t)$. Thus, it has $g_i(\dot{\Theta}(t)) = 0$ and $\beta_i(t) \geq 0$ with $g_i(\dot{\Theta}(t)) + \beta_i(t) \geq 0$. *Case 2:* If $g_i(\dot{\Theta}(t)) + \beta_i(t) \leq 0$, then

$$\digamma_i^+(g_i(\dot{\Theta}(t)) + \beta_i(t)) = \beta_i(t) = 0, \tag{43}$$

which further leads to $g_i(\dot{\Theta}(t)) \leq 0$ with $g_i(\dot{\Theta}(t)) + \beta_i(t) \leq 0$. By summarizing the above two cases, it has:

$$g_i(\dot{\Theta}(t)) = 0, \text{ and } \beta_i(t) \geq 0, \tag{44}$$

and $\beta_i(t) g_i(\dot{\Theta}(t)) = 0$, or

$$g_i(\dot{\Theta}(t)) \leq 0, \text{ and } \beta_i(t) = 0, \tag{45}$$

and further yields:

$$\beta_i(t) g_i(\dot{\Theta}(t)) = 0, \ \forall i = 1, 2, \cdots, p. \tag{46}$$

Thus, one can obtain $\sum_{i=1}^{p} \beta_i(t) g_i(\dot{\Theta}(t)) = 0$ and $\beta^{\mathrm{T}}(t) \mathbf{g}(\dot{\Theta}(t)) = 0$ with $\mathbf{g}(\dot{\Theta}(t)) \leq 0$ and $\beta(t) \geq 0$. Part II completes, and the whole proof is thus completed. □

Theorem 2. *(Global Stability of IECORNN): Assumed that there exist an optimal solution to the motion control problem (8) of mobile robots with both criteria optimization and physical constraints. If a positive design parameter $\zeta > 0$ and a monotonically increasing-odd activation function $\Upsilon(\cdot)$ are utilized, starting from an arbitrary initial neural network state $\mathbf{s}(0)$, then the closed-loop IECORNN (28) is globally stable in the sense of Lyapunov with the first n elements of state $\mathbf{s}(t)$ converges to an exact time-variant solution $\dot{\Theta}^*(t)$ of the motion control problem (8) of mobile robots.*

Proof. As for solving the motion control problem (8) of mobile robots with both criteria optimization and physical constraints, the neurodynamic equation of the closed-loop IECORNN (28) can be written as below:

$$\dot{\epsilon}(t) = -\zeta\Upsilon(\epsilon(t)), \tag{47}$$

and the ith sub-system of (47) is further depicted in

$$\dot{\epsilon}_i(t) = -\zeta\Upsilon(\epsilon_i(t)) \tag{48}$$

with predefined parameter $\zeta > 0$, and $\Upsilon(\cdot)$ being a monotonically increasing-odd activation function with index $i = 1, 2, \cdots, p$. Define a Lyapunov function candidate as

$$L(t) = \frac{\epsilon_i^2(t)}{2}. \tag{49}$$

Note that $L(t)$ is positive definite in view of $L(t) > 0$ for $\epsilon_i(t) \neq 0$, and $L(t) = 0$ for $\epsilon_i(t) = 0$ only. Afterwards, the time derivative of $L(t)$ is calculated:

$$\dot{L}(t) = \frac{\mathrm{d}L(t)}{\mathrm{d}t} = \epsilon_i(t)\dot{\epsilon}_i(t) = -\eta\epsilon_i(t)\Upsilon(\epsilon_i(t)).$$

Due to the fact that $\Upsilon(\cdot)$ is a monotonically increasing-odd activation function, one can readily obtain:

$$-\Upsilon(\epsilon_i(t)) = \Upsilon(-\epsilon_i(t)),$$

which further yields:

$$-\eta\epsilon_i(t)\Upsilon(\epsilon_i(t)) \begin{cases} < 0, \text{ if } \epsilon_i(t) \neq 0, \\ = 0, \text{ if } \epsilon_i(t) = 0. \end{cases}$$

Therefore, it can be asserted the result that $\dot{L}(t)$ is negative definite for time $t \in [0, +\infty)$ with predefined parameter $\zeta > 0$. By applying the Lyapunov stability theory [55], the closed-loop IECORNN (28) is globally stable with each element of the error function $\epsilon_i(t)$ globally converging to 0. That is to say that the first n elements of state $\mathbf{s}(t)$ converges to an exact time-variant solution $\dot{\Theta}^*(t)$ of the motion control problem (8) of mobile robots with both criteria optimization and physical constraints. This completes the proof. □

Theorem 3. *(Exponential Convergence Property of IECORNN): Assumed that there exist an optimal solution to the motion control problem (8) of mobile robot with both criteria optimization and physical constraints. If a positive design parameter $\zeta > 0$ and a linear activation function, i.e., $\Upsilon(\epsilon_i(t)) = \epsilon_i(t)$, are utilized, starting from an arbitrary initial neural network state $\mathbf{s}(0)$, then the first n elements of neural network state $\mathbf{s}(t)$ of the proposed IECORNN (28) is exponentially converges to an exact time-variant solution $\dot{\Theta}^*(t)$ of the motion control problem (8) of mobile robots with both criteria optimization and physical constraints.*

Proof. Consider the the ith sub-system of (47) as below:

$$\dot{\epsilon}_i(t) = -\zeta \Upsilon(\epsilon_i(t)), \tag{50}$$

with a linear activation function, i.e., $\Upsilon(\epsilon_i(t)) = \epsilon_i(t)$, utilized, it readily obtains:

$$\dot{\epsilon}_i(t) = -\zeta \epsilon_i(t), \tag{51}$$

of which the analytical solution is obtained as follows:

$$\epsilon_i(t) = \epsilon_i(0) \exp(-\zeta t), \tag{52}$$

which evidently indicates that each element of error function $\epsilon(t)$ is exponentially converges to zero with convergence rate being the predefined parameter ζ for the proposed IECORNN (28) activated by the linear activation function, with the first n elements of neural network state $\mathbf{s}(t)$ of the IECORNN (28) is exponentially converges to an exact time-variant solution $\dot{\Theta}^*(t)$ of the motion control problem (8) of mobile robots with both criteria optimization and physical constraints. This completes the proof. □

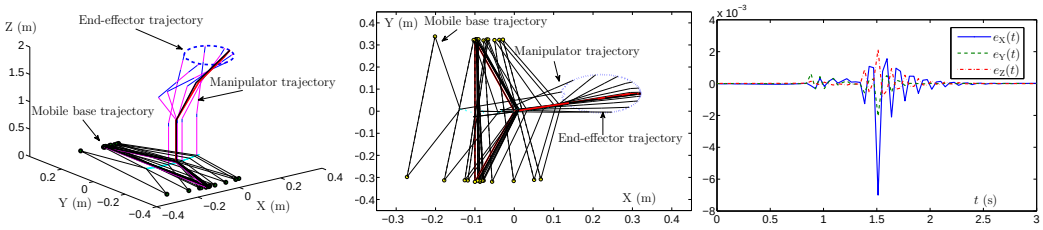

(a) (b) (c)

Figure 2: Motion control results for solving problem (8) of mobile robot with both criteria optimization and physical constraints tracking a circle path via the proposed IECORNN (28). (a) 3D motion trajectories of mobile robots. (b) Top view of motion trajectories of mobile robots. (c) Profile of position error.

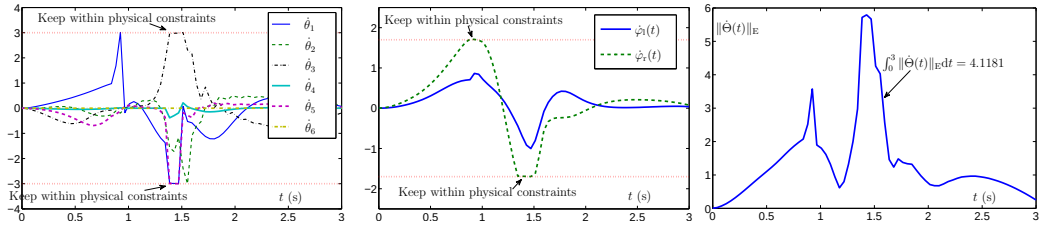

(a) (b) (c)

Figure 3: Motion control signals for solving problem (8) of mobile robot with both criteria optimization and physical constraints tracking a circle path via the proposed IECORNN (28). (a) Profiles of manipulator joint control signals $\dot{\theta}(t)$. (b) Profiles of driving wheels control signals $\dot{\phi}(t)$. (c) Profile of Euclidean norm of control signals $\|\dot{\Theta}(t)\|_{\mathrm{E}}$.

4. Verifications and comparisons

In this section, numerical experiments on the basis of a mobile robot are conducted via two different motion control applications. Then, comprehensive comparisons with existing neural network models, i.e., the CRNN and gradient recurrent neural network (GRNN) are illustrated and investigated. Without losing generality, the initial position of the robot manipulator on the mobile base is set to be $(\mathrm{X_m}(0), \mathrm{Y_m}(0), \mathrm{Z_m}(0)) = (0, 0, 0)$. The initial value of the combined-angle vector of mobile robot is set to be $\dot{\Theta}(0) = [0, 0, \pi/12, \pi/12, \pi/12, \pi/12, \pi/12, \pi/12]^{\mathrm{T}}$ rad. In addition, the initial position vector $\mathbf{r}_{\mathrm{m}}(0)$ of end-effector equipped on the mobile based is set on the starting point of the design path $\mathbf{r}_{\mathrm{md}}(0)$ in the simulations. The mobile robot motion control duration is set to be $T_{\mathrm{d}} = 3$ s. Moreover, the predefined design parameter is set to be $\zeta = 10$, and the activation function

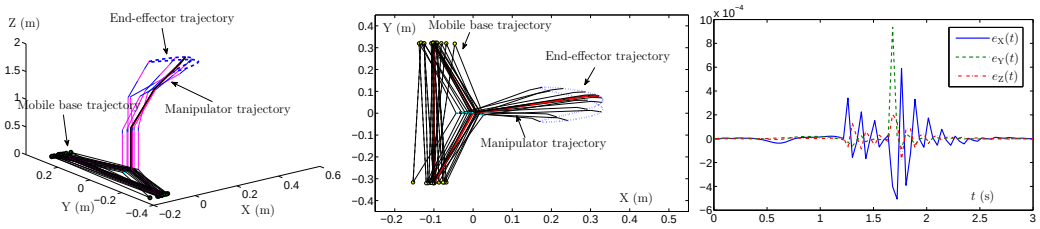

(a) (b) (c)

Figure 4: Motion control results for solving problem (8) of mobile robot with both criteria optimization and physical constraints tracking a Lissajous-shaped path via the proposed IECORNN (28). (a) 3D motion trajectories of mobile robots. (b) Top view of motion trajectories of mobile robots. (c) Profile of position error.

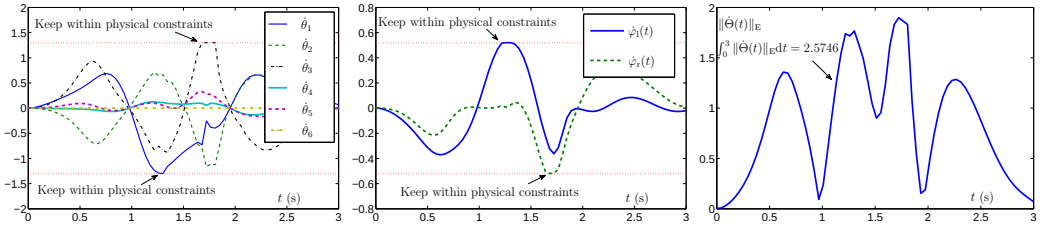

(a) (b) (c)

Figure 5: Motion control signals for solving problem (8) of mobile robot with both criteria optimization and physical constraints tracking a Lissajous-shaped path via the proposed IECORNN (28). (a) Profiles of manipulator joint control signals $\dot{\theta}(t)$. (b) Profiles of driving wheels control signals $\dot{\phi}(t)$. (c) Profile of Euclidean norm of control signals $\|\dot{\Theta}(t)\|_E$.

$\Upsilon(\cdot)$ is set to be the linear activation function throughout the following two motion control applications and comparisons.

4.1. Motion control with circle path tracking

In this motion control application, the end-effector of manipulator is firstly considered to track a circle path with mobile robot considering both criteria optimization and physical constraints as depicted in (8). Note that the upper bound of the physical constraint for joint control signals $\dot{\Theta}(t)$ are set to be $\dot{\Theta}^+ = [1.7, 1.7, 3, 3, 3, 3, 3, 3]$ rad/s. The lower bound of the physical constraint for joint control signals $\dot{\Theta}(t)$ are set to be $\dot{\Theta}^- = -[1.7, 1.7, 3, 3, 3, 3, 3, 3]$ rad/s. The corresponding numerical experiment results for solving problem (8) of mobile robot with both criteria optimization and physical constraints tracking a circle path via the proposed IECORNN (28) are presented in Fig.

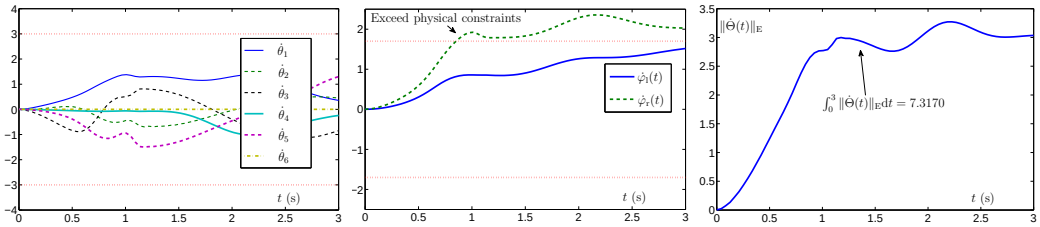

(a) (b) (c)

Figure 6: Comparison results on control signals with both criteria optimization and physical constraints for mobile robot tracking a circle path via existing CRNN (5) compared to the proposed IECORNN (28) in Fig. 3. (a) Profiles of manipulator joint control signals $\dot{\theta}(t)$. (b) Profiles of driving wheels control signals $\dot{\phi}(t)$. (c) Profile of Euclidean norm of control signals $\|\dot{\Theta}(t)\|_{\mathrm{E}}$.

2 and 3. Firstly, one can readily find that in Fig. 2(a) the mobile robot stably achieves the circle path tracking task illustrated via the motion control trajectories in a 3D space. Another top view of the motion control process can be found in Fig. 2(b), which also illustrates the effectiveness of the motion control process. Initially starting from a position, the actual trajectory almost overlaps the desired path during the robot motion task execution. Such results verify that the desired circle path tracking task is completed very well. The small position error shown in Fig. 2(c) also illustrates the high motion control accuracy during the tracking process for mobile robot considering both criteria optimization and physical constraints. Moreover, the related motion control signals for solving problem (8) of mobile robot via the proposed IECORNN (28) are shown in Fig. 3. It can be readily found in Fig. 3(a) that the profiles of manipulator joint control signals $\dot{\theta}(t)$ are strictly constrained by the physical joint velocity limits, which depicted as the inequality constraint during the whole motion control process. In addition, the profiles of driving wheels control signals $\dot{\phi}(t)$ also strictly comply with the physical constraints with upper and lower bound (see Fig. 3(b)). Note that the profile of Euclidean norm of control signals $\|\dot{\Theta}(t)\|_{\mathrm{E}}$ is illustrated in Fig. 3(c) to monitor the integral value of Euclidean norm of control signals during the task execution being $\int_0^3 \|\dot{\Theta}(t)\|_{\mathrm{E}} dt$ which are related to the energy consumption.

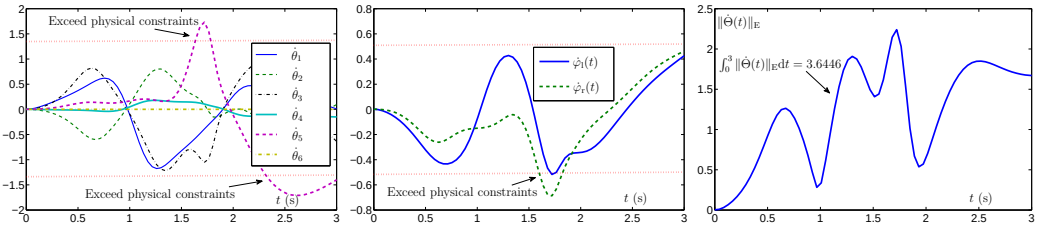

(a) (b) (c)

Figure 7: Comparison results on control signals with both criteria optimization and physical constraints for mobile robot tracking a Lissajous-shaped path via existing CRNN (5) compared to the proposed IECORNN (28) in Fig. 5. (a) Profiles of manipulator joint control signals $\dot{\theta}(t)$. (b) Profiles of driving wheels control signals $\dot{\phi}(t)$. (c) Profile of Euclidean norm of control signals $\|\dot{\Theta}(t)\|_{\mathrm{E}}$.

4.2. Motion control with Lissajous-shaped path tracking

In the second motion control application, we consider the end-effector of manipulator on the mobile robot to track a Lissajous-shaped path in three dimensions space. In this case, the upper bound of physical constraint for joint control signals $\dot{\Theta}(t)$ are set to be $\dot{\Theta}^{+} = [0.52, 0.52, 1.3, 1.3, 1.3, 1.3, 1.3, 1.3]$ rad/s, and the lower bound of physical constraint for joint control signals $\dot{\Theta}(t)$ are set to be $\dot{\Theta}^{-} = -[0.52, 0.52, 1.3, 1.3, 1.3, 1.3, 1.3, 1.3]$ rad/s. The related numerical experiment results for solving problem (8) of mobile robot with both criteria optimization and physical constraints tracking a Lissajous-shaped path via the proposed IECORNN (28) are presented in Fig. 4 and 5. Specifically, it can be readily found that in Fig. 4(a) the mobile robot also stably completes the Lissajous-shaped path tracking task illustrated via the motion control trajectories in a 3D space. Then, the top view of the motion control process is shown in Fig. 4(b), which also illustrates the effectiveness of the motion control process in this case. Initially starting from a position, the actual trajectory almost overlaps the desired path during the robot motion task execution. The results verify that the desired Lissajous-shaped path tracking task is also completed successfully. The small position error shown in Fig. 2(c) demonstrates the high motion control accuracy during the tracking process for mobile robot considering both criteria optimization and physical constraints. Afterward, the motion control signals for solving problem (8) of mobile robot with the objective of Lissajous-shaped path tracking via the proposed IECORNN (28) are shown in Fig. 3. One can readily find that the profiles of manipulator joint control signals $\dot{\theta}(t)$ are also strictly con-

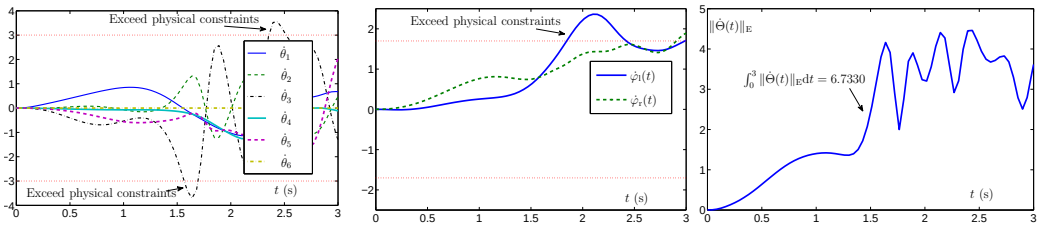

(a) (b) (c)

Figure 8: Comparison results on control signals with both criteria optimization and physical constraints for mobile robot tracking a circle path via existing GRNN (53) compared to the proposed IECORNN (28) in Fig. 3. (a) Profiles of manipulator joint control signals $\dot{\theta}(t)$. (b) Profiles of driving wheels control signals $\dot{\phi}(t)$. (c) Profile of Euclidean norm of control signals $\|\dot{\Theta}(t)\|_{\mathrm{E}}$.

strained by the physical joint velocity limits, which depicted as the inequality constraint during the whole motion control process (see Fig. 5(a)). Besides, the profiles of driving wheels control signals $\dot{\phi}(t)$ also strictly comply with the physical constraints with upper and lower bound (see Fig. 5(b)). The profile of Euclidean norm of control signals $\|\dot{\Theta}(t)\|_{\mathrm{E}}^2$ is illustrated in Fig. 3(c) to monitor the integral value of Euclidean norm of control signals during task execution which are related to the energy consumption in this motion control case.

4.3. Comparisons with CRNN

In the Introduction part and Section 2, the CRNN has been introduced as a conventional solution for solving the motion control of mobile robot. Specifically, for solving the same path tracking control problem (8) of mobile robot, the associated CRNN is depicted as (5), where the value of the predefined design parameter γ is the same as the one ζ of IECORNN (28). Besides, other conditions are set the same as those in Sections 4.1 and 4.2. The comparative results on control signals for mobile robot tracking a circle path as well as Lissajous-shaped path are shown in Figs. 6 and 7. Comparatively, Fig. 6(a) and Fig. 7(a) show that the joint control signals of manipulator $\dot{\theta}(t)$ via the CRNN (5), and those for Lissajous-shaped path-tracking can not comply with the physical constraints with the real-time profiles pass over the upper bound and lower bound during the time instants such as $t \in [1.6, 1.7]$ s and $t \in [2.3, 3.0]$ s, respectively, which are contrary to those results via the proposed IECORNN (28) in Fig. 3(a) and Fig. 5(a). In addition, the profiles

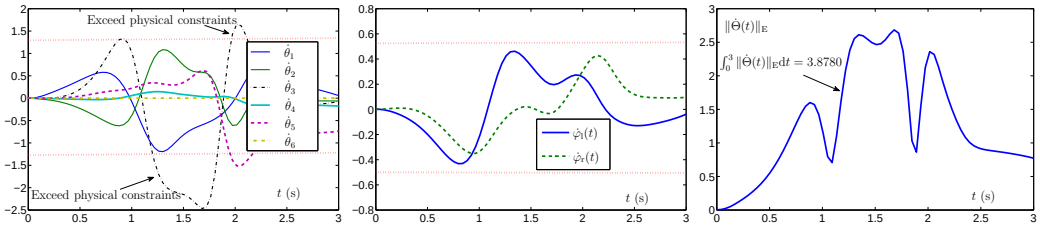

(a) (b) (c)

Figure 9: Comparison results on control signals with both criteria optimization and physical constraints for mobile robot tracking a Lissajous-shaped path via existing GRNN (53) compared to the proposed IECORNN (28) in Fig. 5. (a) Profiles of manipulator joint control signals $\dot{\theta}(t)$. (b) Profiles of driving wheels control signals $\dot{\phi}(t)$. (c) Profile of Euclidean norm of control signals $\|\dot{\Theta}(t)\|_{\mathrm{E}}$.

of driving wheels control signals $\dot{\phi}(t)$ also do not comply with the physical constraints with the real-time profiles pass over the upper bound and lower bound during the time instants such as $t \in [0.8, 3.0]$ s and $t \in [1.6, 1.8]$ s, respectively, which are contrary to those results via the proposed IECORNN (28) in Fig. 3(b) and Fig. 5(b) (see Fig. 6(b) and Fig. 7(b)). Moreover, the integral value of Euclidean norm of control signals with respective to time during the task execution $\int_0^3 \|\dot{\Theta}(t)\|_{\mathrm{E}}^2 \mathrm{d}t$ are comparatively higher than those via the proposed IECORNN (28) in Fig. 3(c) and Fig. 5(c), which illustrates the energy consumption is effectively optimized via the proposed IECORNN (28). The above results verify that the proposed IECORNN (28) is able to consider both criteria optimization and physical constraints is superior to the existing CRNN (5) for mobile robot motion control in practical applications.

4.4. Comparisons with GRNN

As a typical kind of RNN, many GRNNs have been introduced and investigated as a feasible alternative for the online scientific problems solving. Specifically, for solving the time-variant nonlinear optimization problem, a scalar-valued energy function is usually defined as $\mathcal{E}(t) = \|\mathbf{e}(t)\|_{\mathrm{E}}^2/2$. Then, the GRNN can be constructed as follows:

$$\begin{aligned} \dot{\Theta}(t) = -\rho \frac{\partial \mathcal{E}(t)}{\partial \dot{\Theta}(t)} &= -\rho \mathcal{M}^{\mathrm{T}}(\phi(t), \theta(t)) \mathbf{e}(t), \\ &= -\rho \mathcal{M}^{\mathrm{T}}(\phi(t), \theta(t)) (\mathbf{r}_{\mathrm{m}}(t) - \mathbf{r}_{\mathrm{md}}(t)), \end{aligned} \tag{53}$$

where ρ is a predefined parameter for the GRNN. In this comparison, the value of the predefined design parameter ρ is the same as the one ζ of IECORNN

(28) with other conditions being set the same as those in Sections 4.1 and 4.2. The comparative results on control signals via GRNN (53) for mobile robot tracking a circle path as well as Lissajous-shaped path are shown in Figs. 8 and 9. Comparatively, both Fig. 8(a) and Fig. 9(a) show that the joint control signals $\dot{\theta}(t)$ via the GRNN (53) also can not comply with the physical constraints with the real-time profiles pass over the upper bound and lower bound during the time instants such as $t \in [1.6, 1.7]$ s and $t \in [2.4, 2.5]$ s as well as $t \in [1.2, 1.8]$ s and $t \in [2.0, 2.1]$ s, respectively, being contrary to those results via the proposed IECORNN (28) in Fig. 3(a) and Fig. 5(a). The profiles of driving wheels control signals $\dot{\phi}(t)$ also do not comply with the physical constraints with the real-time profiles pass over the upper bound and lower bound during the time instants such as $t \in [1.8, 2.4]$ s and $t \in [2.9, 3.0]$ s, respectively, being contrary to those results via the proposed IECORNN (28) in Fig. 3(b) (see Fig. 8(b) and Fig. 9(b)). Similarly, the integral value of Euclidean norm of control signals with respective to time during the task execution $\int_0^3 \|\dot{\Theta}(t)\|_{\mathrm{E}}^2 \mathrm{d}t$ are comparatively higher than those via the proposed IECORNN (28) in Fig. 3(c) and Fig. 5(c), which illustrates the energy consumption is effectively optimized via the proposed IECORNN (28).

5. Conclusion and future work

Conventional motion control of mobile robots in the unified framework of RNN can not consider both criteria optimization and physical constraints. To overcome this limitation, this paper have has proposed a novel IECORNN to handle the motion control of mobile robot. Firstly, the real-time motion control problem with both criteria optimization and physical constraints has been skillfully converted to a time-variant equality system by leveraging the Lagrange multiplier rule. Then, the detailed design process for the proposed IECORNN (28) has been introduced. Afterward, theoretical analyses on the motion control problem conversion equivalence, global stability and exponential convergence property have been rigorously provided. Moreover, numerical experiment verifications and extensive comparisons on the basis of the mobile robot for two different path-tracking application have sufficiently demonstrated the effectiveness and superiority of the proposed IECORNN (28) for the real-time motion control of mobile robots with both criteria optimization and physical constraints.

Future work lies in the following facts: i) development a complete experimental environment equipped with real mobile robot systems for the physical application of the proposed IECORNN (28); ii) extension and implementation of the proposed IECORNN (28) other type of robot systems such as the parallel robots; and iii) exploitation of other kinds of criteria optimization for mobile robots by using the proposed IECORNN (28).

References

[1] L. Jin, S. Li, B. Hua, M. Liu, A survey on projection neural networks and their applications, Appl. Soft Comput. 76 (2019) 533–544.

[2] R. C. Luo, T. J. Hsiao, Dynamic wireless indoor localization incorporate with autonomous mobile robot based on adaptive signal model fingerprinting approach, IEEE Trans. Ind. Electron. 66 (3) (2019) 1940–1951.

[3] D. Guo, Y. Zhang, Li-function activated ZNN with finite-time convergenceapplied to redundant-manipulator kinematic control via time-varyingJacobian matrix pseudoinversion, Appl. Soft Comput. 24 (2014) 158-168.

[4] B. Liao, W. Liu, Pseudoinverse-type bi-criteria minimization scheme forredundancy resolution of robot manipulators, Robotica 33 (10) (2015)21002113.

[5] W. Ye, Z. Li, C. Yang, J. Sun, C.-Y. Su, R. Lu, Vision-based human tracking control of a wheeled inverted pendulum robot, IEEE Trans. Cybern. 46 (11) (2016) 2423–2434.

[6] K. Li, R. C. Voicu, S. S. Kanhere, W. Ni, E. Tovar, Energy efficient legitimate wireless surveillance of UAV communications, IEEE Trans. Veh. Technol. 68 (3) (2019) 2283–2293.

[7] L. Li, S. Yan, X. Yu, Y. K. Tan, H. Li, Robust multiperson detection and tracking for mobile service and social robots, IEEE Trans. Syst., Man, Cybern. B, Cybern. 42 (5) (2012) 1398–1412.

[8] H. Xiao, Z. Li, C. Yang, L. Zhang, P. Yuan, L. Ding, T. Wang, Robust stabilization of a wheeled mobile robot using model predictive control based on neurodynamics optimization, IEEE Trans. Ind. Electron. 64 (1) (2017) 505–516.

[9] Z. Lim, S. Ponnambalam, I. Kazuhiro, Nature inspired algorithms to optimizerobot work cell layouts, Appl. Soft Comput. 49 (2016) 570–589.

[10] L. Cheng, Z. G. Hou, M. Tan, Adaptive neural network tracking control for manipulators with uncertain kinematics, dynamics and actuator model, Automatica 45 (10) (2009) 2312-2318.

[11] X. Yan, M. Liu, L. Jin, S. Li, B. Hu, X. Zhang, Z. Huang, New zeroing neural network models for solving nonstationary Sylvester equation with verifications on mobile manipulators, IEEE Trans. Ind. Informat. to be published, doi: 10.1109/TII.2019.2899428.

[12] S. Wang, J. Na, X. Ren, RISE-based asymptotic prescribed performance tracking control of nonlinear servo mechanisms, IEEE Trans. Syst., Man, Cybern., Syst. 48 (12) (2018) 2359–2370.

[13] Y. A. Kapitanyuk, A. V. Proskurnikov, M. Cao, A guiding vector-field algorithm for path-following control of nonholonomic mobile robots, IEEE Trans. Control Syst. Technol, 26 (4) (2018) 1372–1385.

[14] B. Siciliano, O. Khatib, Eds. Springer Handbook of Robotics. Berlin, Germany: Springer-Verlag, 2008.

[15] C. Yang, Z. Li, J. Li, Trajectory planning and optimized adaptive control for a class of wheeled inverted pendulum vehicle models, IEEE Trans. Cybern. 43 (1) (2013) 24–36.

[16] Y. Zhang, X. Yan, D. Chen, D. Guo, W. Li, QP-based refined manipulability-maximizing scheme for coordinated motion planning and control of physically constrained wheeled mobile redundant manipulators, Nonlinear Dyn. 85 (1) (2016) 245–261.

[17] D. Chen, Y. Zhang, A hybrid multi-objective scheme applied to redundant robot manipulators, IEEE Trans. Autom. Sci. Eng. 14 (7) (2017) 1337–1350.

[18] D. Chen, Y. Zhang, Robust zeroing neural-dynamics and its time-varying disturbances suppression model applied to mobile robot manipulators, IEEE Trans. Neural Netw. Learn. Syst. 29 (9) (2018) 4385–4397.

[19] Z. Zhang, Z. Li, Y. Zhang, Y. Luo, Y. Li, Neural-dynamic-method-based dual-arm CMG scheme with time-varying constraints applied to humanoid robots, IEEE Trans. Neural Netw. Learn. Syst. 26 (12) (2015) 3251–3262.

[20] Z. Li, B. Liao , F. Xu, D. Guo, A new repetitive motion planning scheme with noise suppression capability for redundant robot manipulators, IEEE Trans. Syst., Man, Cybern., Syst. to be published, doi: 10.1109/TSMC.2018.2870523.

[21] D. Guo, Y. Zhang, Simulation and experimental verification of weighted velocity and acceleration minimization for robotic redundancy resolution, IEEE Trans. Autom. Sci. Eng. 11 (4) (2014) 1203–1217.

[22] Y. Zhang, J. Wang, Y. Xia, A dual neural network for redundancy resolution of kinematically redundant manipulators subject to joint limits and joint velocity limits, IEEE Trans. Neural Netw. 14 (3) (2003) 658667.

[23] Y. Zhang, S. Li, J. Gui, X. Luo, Velocity-level control with compliance to acceleration-level constraints: a novel scheme for manipulator redundancy resolution, IEEE Trans. Ind. Informat. 14 (3) (2018) 921–930.

[24] D. Chen, Y. Zhang, Minimum jerk norm scheme applied to obstacle avoidance of redundant robot arm with jerk bounded and feedback control, IET Control Theo. Appl. 10 (15) (2016) 1896–1903.

[25] Z. Zhang, Y. Zhang, Variable joint-velocity limits of redundant robot manipulators handled by quadratic programming, IEEE/ASME Trans. Mechatronics 18 (2) (2013) 674–686.

[26] L. Xiao, A nonlinearly-activated neurodynamic model and its finite-timesolution to equality-constrained quadratic optimization with nonstationarycoefficients, Appl. Soft Comput. 40 (2016) 252–259.

[27] L. Jin, S. Li, H. Wang, Z. Zhang,Nonconvex projection activated zeroing neurodynamic models for time-varying matrix pseudoinversion with accelerated finite-time convergence, Appl. Soft Comput. 62 (2018) 840-850.

[28] C. Yang, C. Chen, W. He, R. Cui, Z. Li, Robot learning system based on adaptive neural control and dynamic movement primitives, IEEE Trans. Neural Netw. Learn. Syst. 30 (3) (2019) 777–787.

[29] D. Wang, H. He, D. Liu, Adaptive critic nonlinear robust control: a survey, IEEE Trans. Cybern. 47 (10) (2017) 3429–3451.

[30] Q. Wei, D. Liu, Q. Lin, R. Song, Adaptive dynamic programming for discrete-time zero-sum games, IEEE Trans. Neural Netw. Learn. Syst. 29 (4) (2018) 957–969.

[31] Y.-J. Liu, M. Gong, S. Tong, C. L. P. Chen, D.-J. Li, Adaptive fuzzy output feedback control for a class of nonlinear systems with full state constraints, IEEE Trans. Fuzzy Syst. 26 (5) (2018) 2607–2617.

[32] B. Luo, D. Liu, T. Huang, D. Wang, Model-free optimal tracking control via critic-only Q-learning, IEEE Trans. Neural Netw. Learn. Syst. 27 (10) (2016) 2134–2144.

[33] Y.-J. Liu, S. Tong, D.-J. Li, Y. Gao, Fuzzy adaptive control with state observer for a class of nonlinear discrete-time systems with input constraint, IEEE Trans. Fuzzy Syst. 24 (5) (2016) 1147–1158.

[34] D. Chen, Y. Zhang, S. Li, Tracking control of robot manipulators with unknown models: a Jacobian-matrix-adaption method, IEEE Trans. Ind. Informat. 14 (7) (2018) 3044–3053.

[35] Y. Zhang, S. Li, Perturbing consensus for complexity: a finite-time discrete biased min-consensus under time-delay and asynchronism, Automatica 85 (2017) 441–447.

[36] J. Na, Y. Huang, X. Wu, G. Gao, G. Herrmann, J. Z. Jiang, Active adaptive estimation and control for vehicle suspensions with prescribed performance, IEEE Trans. Control Syst. Technol 26 (6) (2018) 2063–2077.

[37] Y.-J. Liu, S. Lu, S. Tong, Neural network controller design for an uncertain robot with time-varying output constraint, IEEE Trans. Syst., Man, Cybern., Syst. 47 (8) (2017) 2060–2068.

[38] R. Chandra, S. Chand, Evaluation of co-evolutionary neural networkarchitectures for time series prediction with mobile application in finance,Appl. Soft Comput. 49 (2016) 462–473.

[39] S. Li, M. Zhou, X. Luo, Z. You, Distributed winner-take-all in dynamic networks, IEEE Trans. Autom. Control, 62 (2) (2017) 577–589.

[40] Z. Zhang, L. Zheng, J. Yu, Y. Li, Z. Yu, Three recurrent neural networks and three numerical methods for solving repetitive motion planning scheme of redundant robot manipulators, IEEE/ASME Trans. Mechatronics 22 (3) (2017) 1423–1434.

[41] W. Li, A recurrent neural network with explicitly definable convergence time for solving time-variant linear matrix equations, IEEE Trans. Ind. Informat. to be published, doi: 10.1109/TII.2018.2817203.

[42] W. Li, Z. Su, Z. Tan, A recurrent neural network with explicitly definable convergence time for solving time-variant linear matrix equations, IEEE Trans. Ind. Informat. DOI: 10.1109/TII.2019.2897803.

[43] L. Liu, A. Wu, Z. Zeng, T. Huang, Global mean square exponential stability of stochastic neural networks with retarded and advanced argument, Neurocomputing 247 (2017) 156–164.

[44] S. Li, Z.-H. You, H. Guo, X. Luo, Z.-Q. Zhao, Inverse-free extreme learning machine with optimal information updating, IEEE Trans. Cybern. 46 (5) (2016) 1229–1241.

[45] X. Li, R. Rakkiyappan, G. Velmurugan, Dissipativity analysis ofmemristor-based complex-valued neural networks with time-varying delays,Inf. Sci. 294 (2015) 645–665.

[46] X. Li, M. Bohner, C. Wang, Impulsive differential equations: periodic solutionsand applications, Automatica 52 (2015) 173–178.

[47] W. Li, Design and analysis of a novel finite-time convergent and noise-tolerant recurrent neural network for time-variant matrix inversion, IEEE Trans. Syst., Man, Cybern., Syst. to be published, doi: 10.1109/TSMC.2018.2853598.

[48] H. Lu, L. Jin, X. Luo, B. Liao, D. Guo, L. Xiao, RNN for solving perturbed time-varying underdetermined linear system with double bound limits on residual errors and state variables, IEEE Trans. Ind. Informat. to be published, doi: 10.1109/TII.2019.2909142.

[49] L. Xiao , K. Li, M. Duan, Computing time-varying quadratic optimization with finite-time convergence and noise tolerance: a unified framework

for zeroing neural network, IEEE Trans. Neural Netw. Learn. Syst. to be published, doi: 10.1109/TNNLS.2019.2891252.

[50] L. Xiao, Accelerating a recurrent neural network to finite-time convergence using a new design formula and its application to time-varying matrix square root, J. Franklin Inst. 354 (13) (2017) 5667–5677.

[51] J. H. Mathews, K. K. Fink, Numerical Methods Using MATLAB. Englewood Cliffs, NJ, USA: Prentice-Hall, 2004.

[52] Y. Zhang, L. Xiao, Z. Xiao, M. Mao, Zeroing Dynamics, Gradient Dynamics, and Newton Iterations. Boca Raton, FL, USA: CRC Press, 2015.

[53] X. Huang, X. Lou, B. Cui, A novel neural network for solving convex quadratic programming problems subject to equality and inequality constraints, Neurocomputing 214 (2016) 23–31.

[54] S. Boyd, L. Vandenberghe, Convex Optimization, Cambridge University Press, New York, 2004.

[55] Y.-J. Liu, S. Lu, S. Tong, X. Chen, C. L. Philip Chen, D.-J. Li, Adaptive control-based barrier Lyapunov functions for a class of stochastic nonlinear systems with full state constraints, Automatica 87 (2018) 83–93.